

Supplementary Information for

Bridge-arched and layer-structured hollow melamine foam/reduced graphene oxide composite with enlarged evaporation area and superior thermal insulation for high-performance solar steam generation

Sen Meng, Xing Zhao, Chun-Yan Tang, Peng Yu, Rui-Ying Bao, Zheng-Ying Liu, Ming-Bo

Yang, Wei Yang*

College of Polymer Science and Engineering, Sichuan University, State Key Laboratory of

Polymer Materials Engineering, Chengdu, 610065, Sichuan, China

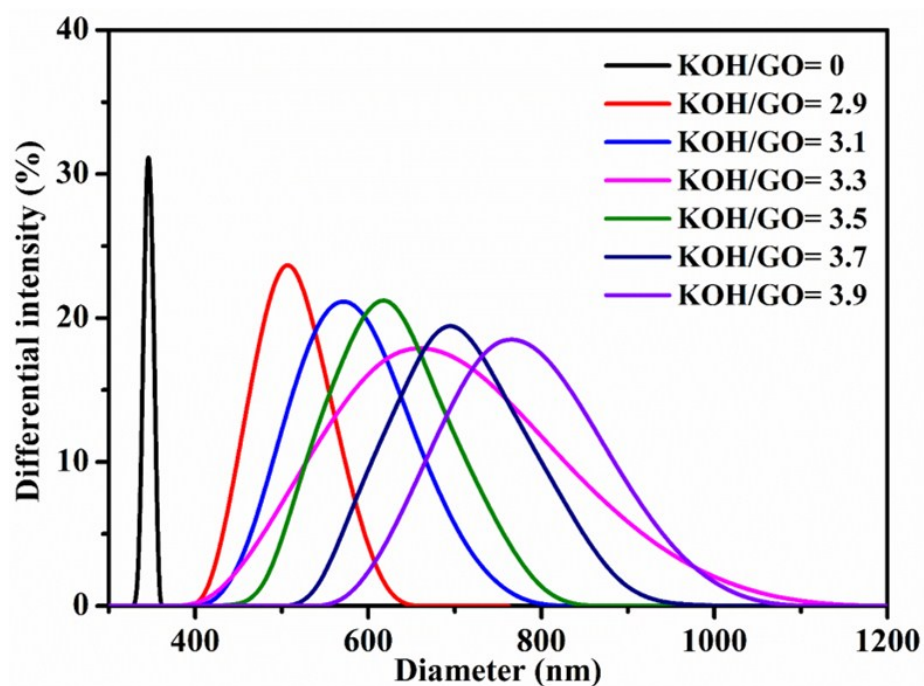


Fig. S1 DLS spectra of GO nanosheets in deionized water with different content of KOH.

*Corresponding author. Tel.: + 86 28 8546 0130; fax: + 86 28 8546 0130.

E-mail address: weiyang@scu.edu.cn (W Yang)

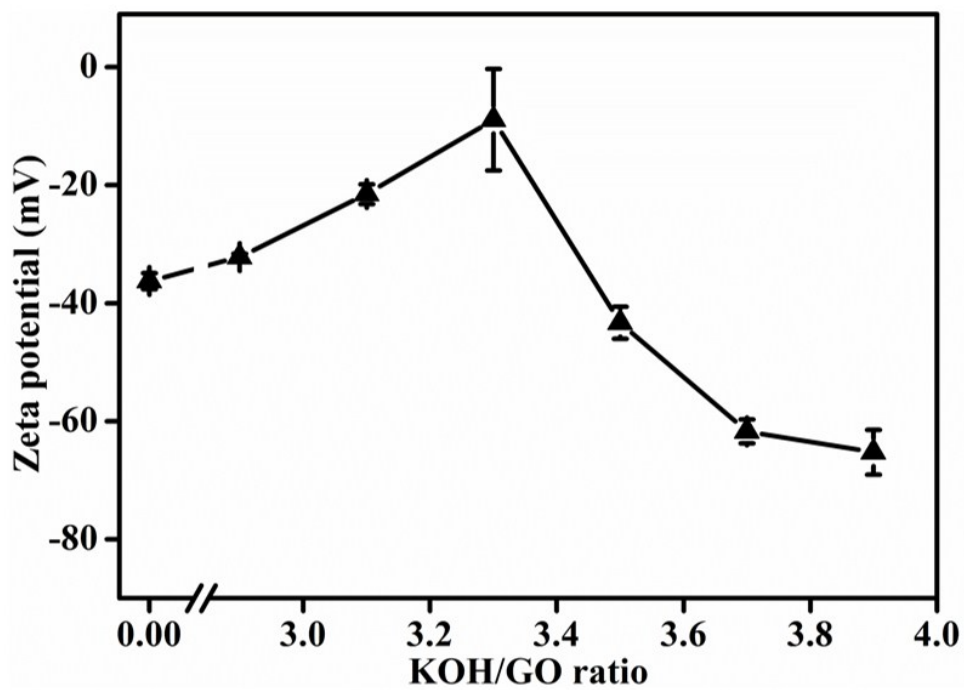


Fig. S2 Zeta potential of GO nanosheets in deionized water with different content of KOH.

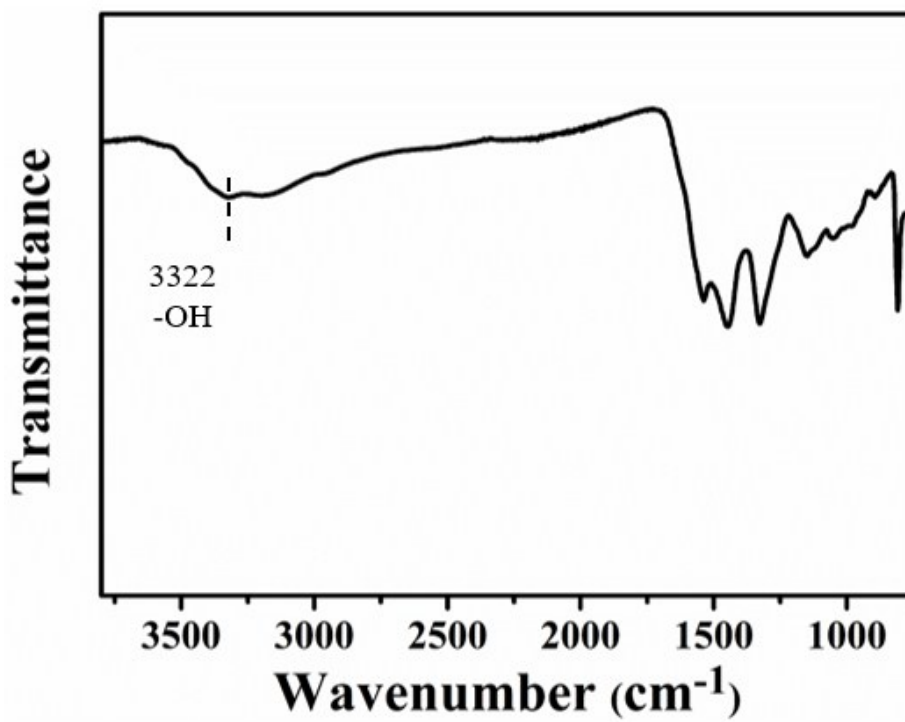
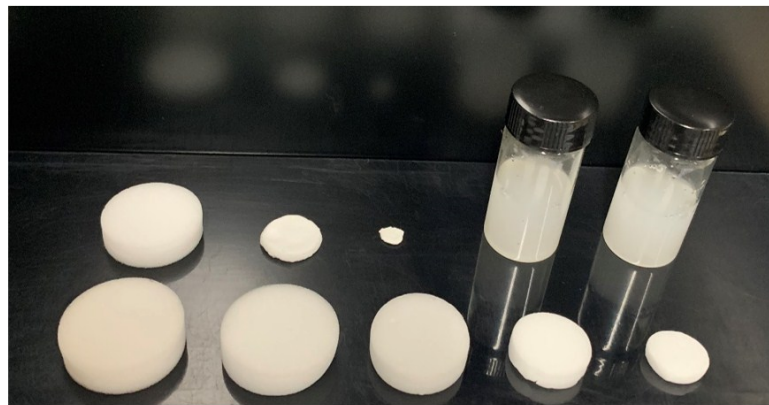
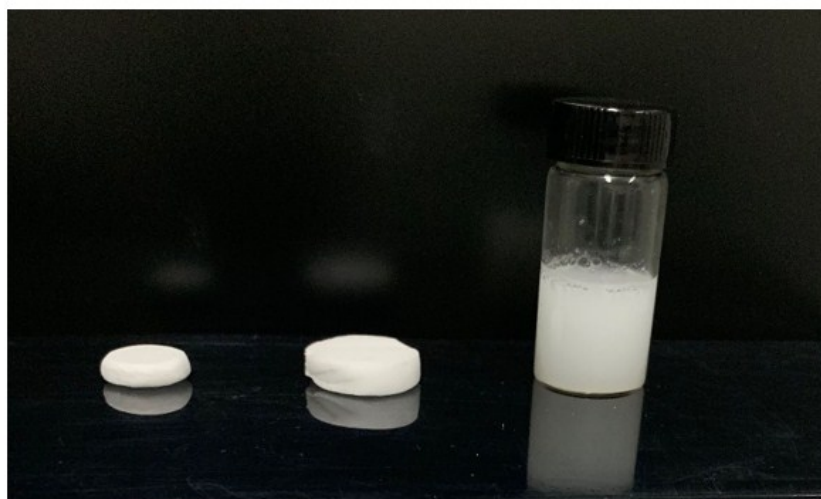


Fig. S3 FTIR spectra of BHMg.



<u>MF+water</u> 1h	MF+water 2h	<u>MF+water</u> 3h	<u>MF+water</u> 4h	<u>MF+water</u> 5h
MF+KOH 1h	MF+KOH 2h	MF+KOH 3h	MF+KOH 4h	MF+KOH 5h

Fig. S4 Photograph of MF hydrothermally treated in water with/without KOH for different time at 180 °C



KOH | NaOH | KCl

Fig. S5 Photograph of MF hydrothermally treated for 5 hours in water with KOH/NaOH/KCl at 180 °C.

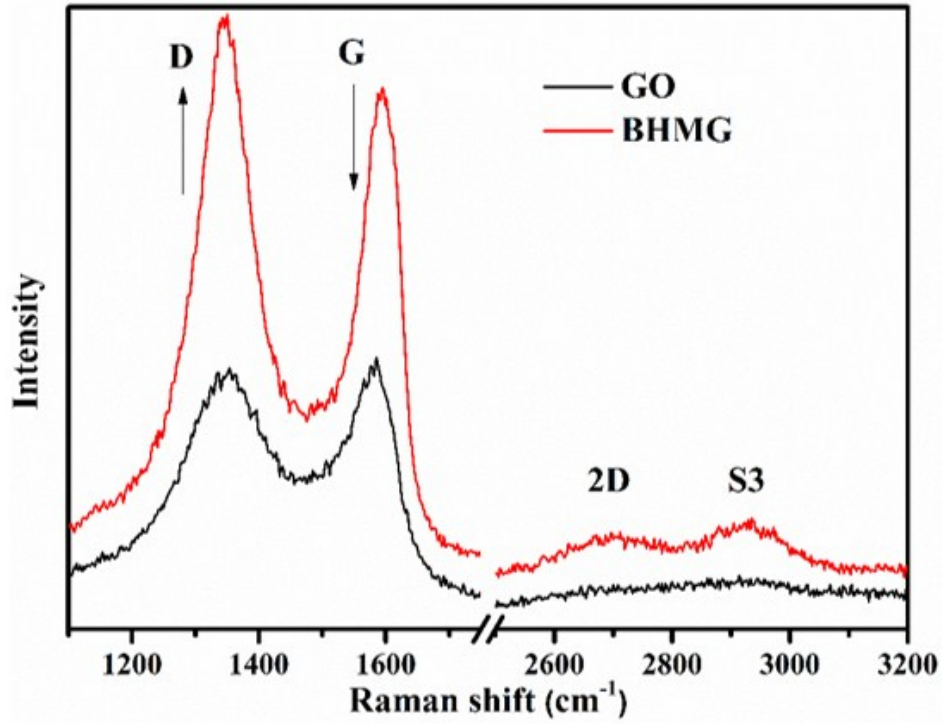


Fig. S6 Micro-Raman spectra of GO (black) and BHMG (red).

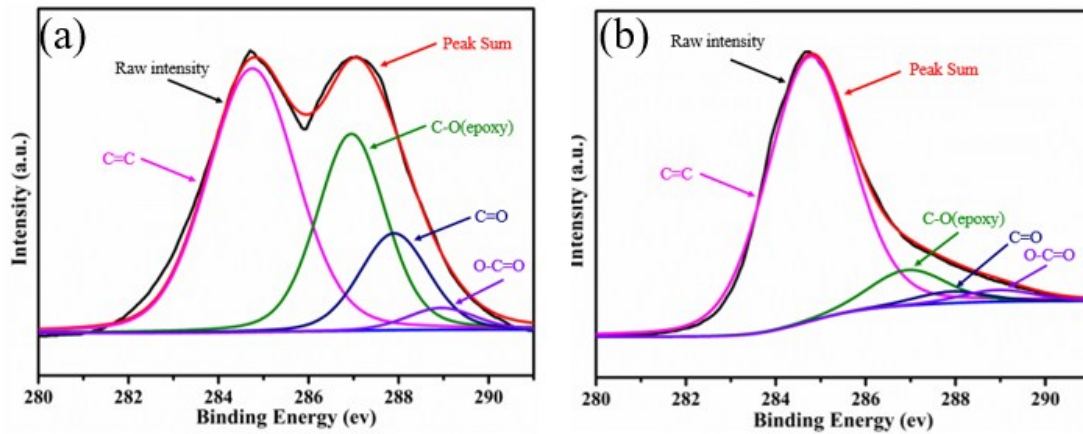


Fig. S7 The C1s XPS spectra of GO (a) and BHMG (b).

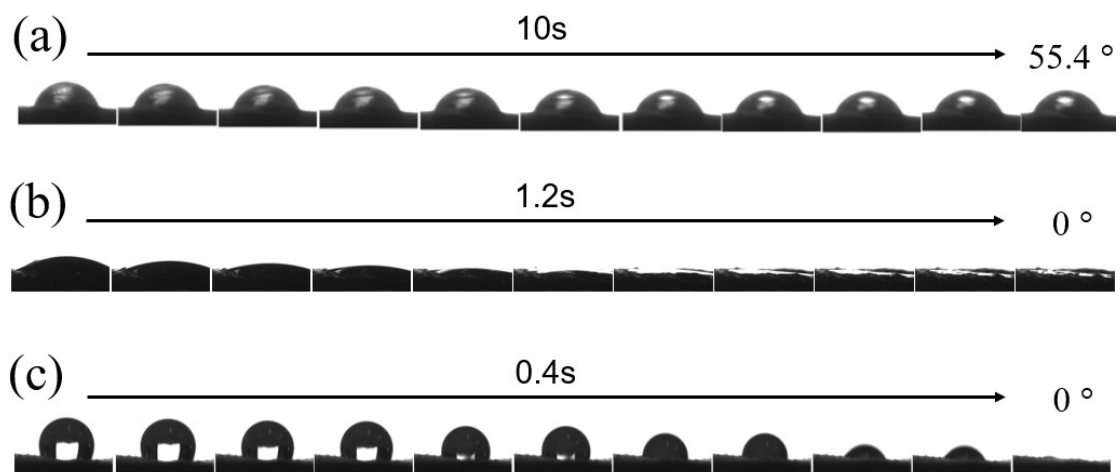


Fig. S8 Contact angle measurement diagram of the raised upper surface, subface and internal surface of BHMg



Fig. S9 Digital images of the sample placed on the surface of water.

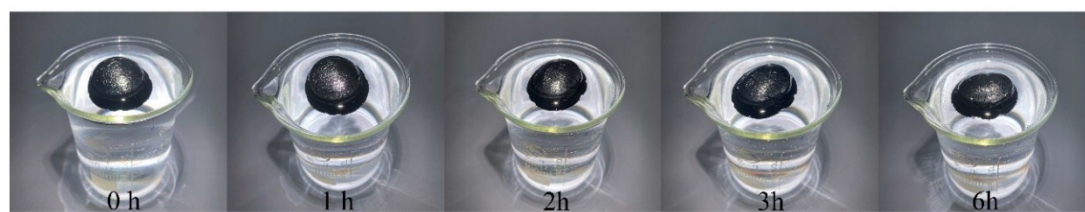


Fig. S10 Digital images of the sample under one sun illumination for different time.



Fig. S11 Photograph of BHMG self-floating on the surface of water.

Section S1. The evaporation efficiency analysis of BHMG solar steam generation device.

The raised surface of the sample is similar to the part of a sphere (spherical crown), the area of the spherical crown is mainly calculated by equation:

$$A_{\text{raised}} = \pi(r^2 + h^2)$$

And r (12.5 mm) is the radius of the circle with the largest opening of the spherical crown. h is the height of the spherical crown. So, the $A_{\text{raised}} \approx 569 \text{ mm}^2$.

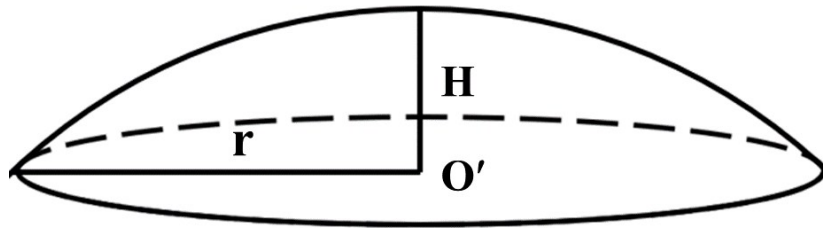


Fig. S12 Schematic diagram of spherical crown.

The projection area of the sample is calculated by equation:

$$A_{\text{projection}} = \pi r^2$$

So, the $A_{\text{projection}} \approx 490 \text{ mm}^2$.

The effect of increasing evaporation area can be described by formula

$$\frac{A_{\text{raised}}}{A_{\text{projection}}} = \frac{\pi(r^2 + h^2)}{\pi r^2} = \frac{r^2 + h^2}{r^2}$$

Thus, we can calculate that $A_{\text{raised}} / A_{\text{projection}}$ is about 1.16. In addition, due to the surface amplification effect of

the integrated evaporator, the solar steam efficiency of 92.9 % can be achieved.

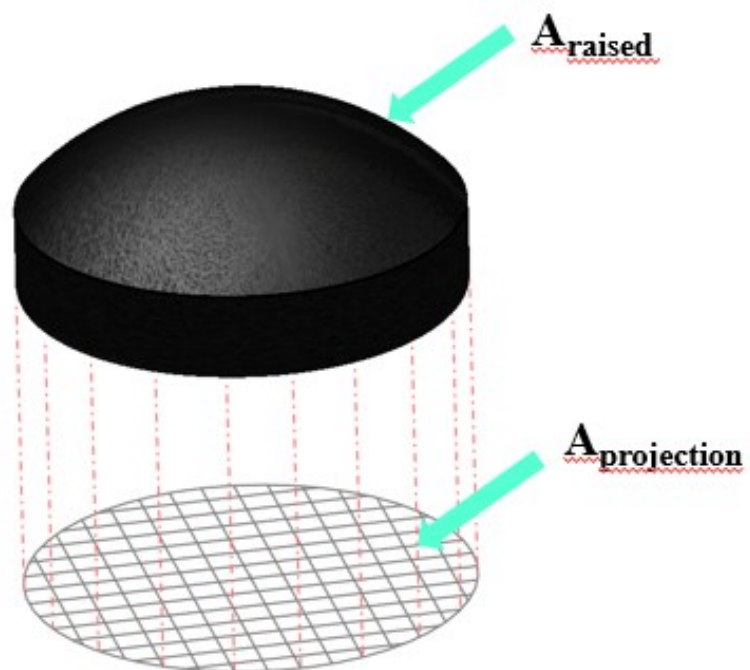


Fig. S13 Schematic diagram of BHM absorber model and projection area.



Fig. S14 Photograph of the BHM absorber with 20 g weight on it



Fig. S15 Photograph of the home-made condensed water collecting device.

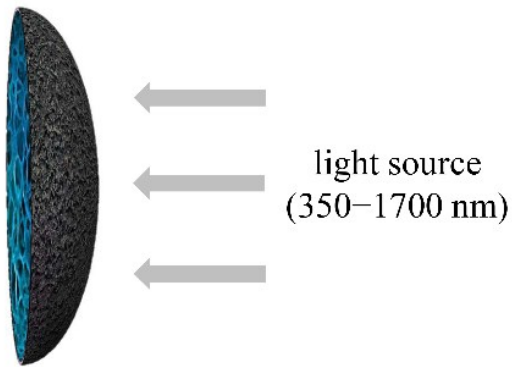


Fig. S16 Schematic diagram of the light absorption measured.

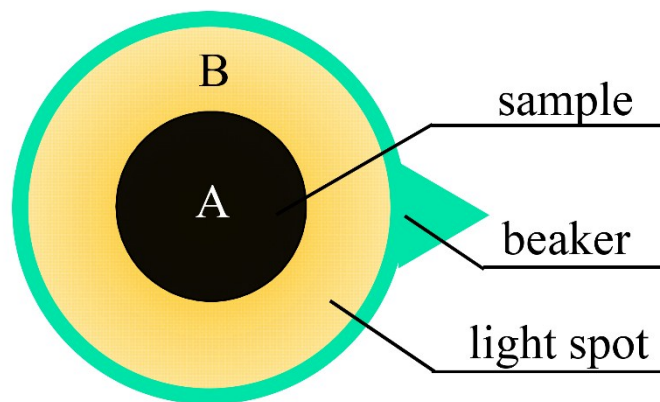


Fig. S17 Schematic diagram of the distribution of light spot.

Table S1. Light power density settings and statistics (partial data)

Sun	Randomly take 14 spots in the center of the light spot (region A) (mw/cm ²)							Average
1	97.9	101.4	96.0	97.9	93.5	97.9	98.3	96.2
	101.0	90.3	92.5	89.9	97.9	94.9	96.7	
Sun	Randomly take 14 spots on the edge of the light spot (region B) (mw/cm ²)							Average
1	7.9	7.4	11.1	13.7	8.0	7.8	9.3	9.9
	10.6	9.0	9.5	8.4	12.3	12.1	11.6	